Comparative Biochemistry and Physiology, Part C 219 (2019) 95–102

Contents lists available at ScienceDirect

Comparative Biochemistry and Physiology, Part C

journal homepage: www.elsevier.com/locate/cbpc

In vivo immunomodulatory and antioxidant properties of nanoceria ($nCeO_2$) in the marine mussel *Mytilus galloprovincialis*

M. Auguste[a,*], T. Balbi[a], M. Montagna[a], R. Fabbri[a], M. Sendra[b], J. Blasco[b], L. Canesi[a]

[a] Dept. of Earth, Environment and Life Sciences (DISTAV), University of Genoa, Genoa, Italy
[b] ICMAN-CSIC, Cadiz, Spain

ARTICLE INFO

Keywords:
$nCeO_2$
Mytilus
Immunity
Antioxidant defenses
Gene expression
Embryos

ABSTRACT

Cerium nanoparticles ($nCeO_2$) are increasingly utilized in a wide variety of industrial, environmental and biomedical applications, and are therefore expected to be released in the aquatic environment. Due to its peculiar redox properties, $nCeO_2$ may present unique hazards to environmental and human health. Previous data showed that in the hemocytes of the marine bivalve *Mytilus galloprovincialis*, *in vitro* exposure to a particular type of $nCeO_2$ (9 nm, characterized by negative ζ-potential, high H_2O_2 scavenging capacity and Ce^{3+}/Ce^{4+} surface ratio) reduced basal ROS production, lysosomal membrane stability and phagocytic activity in the presence of hemolymph serum; the effects observed were partly ascribed to the formation of a SOD-protein corona in the hemolymph.

In this work, the *in vivo* effects of this type of $nCeO_2$ were investigated in mussels exposed to 100 µg/L $nCeO_2$ for 96 h; several lysosomal, immune, inflammatory and antioxidant biomarkers were measured at cellular (hemocytes) and tissue (gills, digestive gland) level. Molecular responses were evaluated in hemocytes and digestive gland by determining expression of 11 selected genes related to known biological functions. The results show specific immunomodulatory and antioxidant effects of $nCeO_2$ at different levels of biological organization in the absence of Cerium tissue accumulation. These data further support the redox mechanisms at the basis of the physiological effects of $nCeO_2$. Finally, in order to evaluate the possible impact at the whole organism level, the effects of $nCeO_2$ were evaluated in the 48 h embryotoxicity assay in a wide concentration range. However, $nCeO_2$ exposure resulted in a small reduction in normal embryo development. Overall, the results demonstrate that in mussels $nCeO_2$ can selectively modulate different physiological processes at different levels of biological organization.

1. Introduction

Manufactured ceria nanomaterials ($nCeO_2$), due to their multiple properties, are increasingly utilized in a wide variety of beneficial industrial, environmental applications, consumer products, and more recently, in biomedical applications due to their catalytic properties and capacity for storing oxygen and scavenging reactive oxygen species (ROS) (Celardo et al., 2011; Reed et al., 2014; Rajeshkumar and Naik, 2018). Global annual production of $nCeO_2$ was estimated at 9.1 kt in 2016 and to progressively increase by 2025 (MRR-Market Research Report, 2017), and expected to be released in many natural compartments. According to the flow model of Gottschalk et al. (2015) the predicted environmental concentration-PEC of $nCeO_2$ are at pg/L levels in freshwater and seawater, and in the range of 44–2300 µg/kg in sewage treatment sludge.

$nCeO_2$ may present unique hazards to environmental and human health, thus increasing concern about their potential safety aspects (Collin et al., 2014; Yokel et al., 2014). Of critical importance are the redox properties of ceria that enables its transition between Ce (III) and Ce (IV), which are the key to understanding its interactions with biological systems. Several reports in mammalian cell lines indicate that $nCeO_2$ induce a protective cellular response acting as a free radical scavenger (Xia et al., 2008) and can exhibit antioxidant mimetic activities/properties (Korsvik et al., 2007; Nelson et al., 2016; Li et al., 2018 and references therein). $nCeO_2$, due to their unusual electron configurations and redox capacity, may also participate in several other biological processes, such as interactions with cell membranes or energy transduction pathways that have the potential to cause harmful effects at high enough concentrations or over long time scales. However, hypotheses on the precise cause of the mechanism of possible

* Corresponding author at: DISTAV, University of Genoa, Palazzo delle Scienze 26, 16132 Genoa, Italy.
E-mail address: manon.auguste@edu.unige.it (M. Auguste).

https://doi.org/10.1016/j.cbpc.2019.02.006
Received 21 November 2018; Received in revised form 9 January 2019; Accepted 15 February 2019
Available online 21 February 2019

interactions of nanoceria with biological systems *in vivo* are still speculative (Conway et al., 2014).

Aquatic ecotoxicity data based on EC_{50} values indicate no adverse effects below 10 μg/L, a concentration much higher than the maximum PECs in aquatic compartments (O'Brien and Cummins, 2010; Collin et al., 2014; Taylor et al., 2015 and references quoted therein). However, information is scanty on the sublethal effects and potential mechanism of action of $nCeO_2$ in aquatic organisms. Among these, bivalve molluscs, as suspension-feeders, have been shown to represent significant targets for different types NPs, that can trap these NP particles/aggregates formed in aquatic media through the gill sieve (Canesi et al., 2012). The *in vivo* effects of $nCeO_2$ have been investigated in bivalves, usually utilized in biomonitoring of aquatic ecosystems, in terms of uptake/accumulation (Montes et al., 2012; Conway et al., 2014) and evaluation of biomarker responses (Garaud et al., 2015; Koehlé-Divo et al., 2018). Overall, these data indicate that, although little bioconcentration of cerium occurs in bivalves, $nCeO_2$ can affect several biomarkers, including the activity of antioxidant enzymes. However, no information is available on the effects of $nCeO_2$ on the immune function, on the possible molecular mechanisms underlying the effects measured at tissue level, or possible impacts at the whole organism level.

In the marine mussel *Mytilus galloprovincialis*, the effects and mechanisms of action of different $nCeO_2$ types have been previously investigated *in vitro* in the immune cells, the hemocytes. The results showed specific effects depending on physico-chemical characteristics of primary particles and secondary characteristics due to transformation and behavior of $nCeO_2$ in exposure media (Ciacci et al., 2012; Canesi et al., 2017; Sendra et al., 2018). In particular, hemocyte exposure to one type of $nCeO_2$ (9 ± 4 nm, with negative zeta potential, rounded shape, high H_2O_2 scavenging capacity and Ce^{3+}/Ce^{4+} surface ratio), in the presence of hemolymph serum (HS) reduced basal oxyradical (ROS) production and induced stronger effects on lysosomal and immune parameters, with respect to those observed in the presence of artificial sea water-ASW (Canesi et al., 2017; Sendra et al., 2018). The effects were partly ascribed to the capacity of this type of $nCeO_2$ to specifically interact with extracellular SOD (superoxide dismutase) forming a protein corona in HS (Canesi et al., 2017).

However, the results obtained *in vitro* do not necessarily reflect the possible impact of *in vivo* exposure to NPs. In the surrounding environment, NP interactions with polysaccharides, proteins and colloids may affect their agglomeration/aggregation and consequent bioavailability (Canesi and Corsi, 2016). Moreover, once within the organism, different NPs may specifically bind to plasma proteins, forming a protein corona that can affect particle uptake and toxicity in target cells (Canesi et al., 2017).

In this work, the effects of the same type of $nCeO_2$ utilized in *in vitro* experiments described above (Canesi et al., 2017; Sendra et al., 2018) were evaluated *in vivo*, in mussels exposed to 100 μg/L $nCeO_2$ for 96 h, and several lysosomal, immune, inflammatory and antioxidant parameters were measured at cellular (hemocytes) and tissue (gills, digestive gland) level. Molecular responses were evaluated in hemocytes and digestive gland by determining expression of 11 selected genes related to known biological functions, including immune and antioxidant response. Finally, in order to evaluate the possible impact at the whole organism level, the effects of $nCeO_2$ were evaluated in the 48 h embryotoxicity assay in a wide concentration range (0.1–1000 μg/L).

2. Methods

2.1. Characterization of nanoceria

The $nCeO_2$ used within this work (CAS# US7110, with 20% H_2O by wt., obtained from US Research Nanomaterials, Inc.), has been previously studied for interactions with microalgae (Sendra et al., 2017), *in vitro* effects on *Mytilus* hemocytes and corona formation within *Mytilus* hemolymph (Canesi et al., 2017; Sendra et al., 2018). This type of nanoceria (also referred as CNP2 in previous studies) has been thoroughly characterized for the physico-chemical properties of primary particles and behavior in exposure media (water, natural and artificial sea water, *Mytilus* hemolymph serum) and the results are summarized Table S1. For further details, see references above.

2.2. Animals and treatments

Mussels (*M. galloprovincialis* Lam.), purchased in July 2017 from an aquaculture farm (Arborea-OR, Italy), 4–5 cm long, were transferred to the laboratory and acclimatized for 24 h in static tanks containing aerated artificial sea water-ASW (ASTM, 2004), pH 7.9–8.1, 36 ppt salinity (1 L/animal), at 18 ± 1 °C.

Animals (four groups of 12–15 mussels each) were exposed 96 h to $nCeO_2$ at the concentration of 100 μg/L. Experimental tanks were contaminated daily by the addition of aliquots of freshly prepared $nCeO_2$ suspensions in milliQ water (10 mg/L) prepared by bath sonication for 30 min and immediately spiked in the tanks in order to reach the desired concentration. ASW was changed each day and addition of the $nCeO_2$ was immediately after ASW renovation. Parallel groups of control (untreated) mussels were kept in clean ASW. Animals were not fed during the experiments. No mortality was observed in different experimental conditions.

At the end of the exposure, hemolymph was extracted from the adductor muscle of animals, using a syringe with an 18 G1/2″ needle, filtered with gauze, and pooled, at 16 °C. To evaluate biomarkers at tissue levels, gills and digestive glands from 4 groups of mussels were rapidly dissected, pooled, frozen in liquid nitrogen and maintained at −80 °C for further analysis. For histological analyses (lipofuscin content), 5 digestive glands were placed on aluminium chucks, immersed in hexane pre-cooled to −70 °C in liquid nitrogen and maintained at −80 °C (Moore, 1988).

2.3. Hemolymph immune parameters

Hemocyte functional parameters (lysosomal membrane stability-LMS, phagocytosis, extracellular oxyradical production, nitric oxide production) and serum lysozyme activity were evaluated essentially as previously described (Canesi et al., 2010, 2014; Balbi et al., 2014; Barmo et al., 2013).

LMS was evaluated by the NRR (Neutral Red Retention time) assay as previously described (Canesi et al., 2010, 2014; Balbi et al., 2014; Barmo et al., 2013). Hemocyte monolayers on glass slides were incubated with 20 μL of neutral red (NR) solution (final concentration 40 μg/mL from a stock solution of NR 40 mg/mL in DMSO); after 15 min excess dye was washed out and 20 μL of ASW was added. Every 15 min, slides were examined under an optical microscope and the percentage of cells showing loss of the dye from lysosomes in each field was evaluated. For each time point 10 fields were randomly observed, each containing 8–10 cells. The end point of the assay was defined as the time at which 50% of the cells showed sign of lysosomal leaking (the cytosol becoming red and the cells rounded). All incubations were carried out at 16 °C.

Phagocytic activity was evaluated as uptake of Neutral Red-conjugated zymosan particles in hemocyte monolayers as previously described (Barmo et al., 2013). Neutral Red-stained zymosan in 0.05 M Tris-HCl buffer (TBS), pH 7.6, containing 2.5% NaCl was added to each monolayer at a concentration of about 1:50 hemocytes:zymosan diluted in filtered ASW, and allowed to incubate for 60 min at 16 °C. Monolayers were then washed three times with ASW, fixed with Baker's formol calcium (4% *v*/v formaldehyde, 2%NaCl, 1% calcium acetate) for 30 min and mounted in Kaiser's medium for microscopical examination with an inverted Olympus IX53 microscope (Olympus, Milano, Italy). For each slide, the percentage of phagocytic hemocytes was calculated from a minimum of 200 cells. Data are expressed as % of

phagocytizing cells.

Extracellular generation of superoxide by hemocytes was measured by the reduction of cytochrome *c*. Hemolymph was extracted and aliquots (500 µL) of hemocyte suspension in triplicate were incubated with 500 µL of cytochrome *c* solution (75 mM ferricytochrome c in TBS). Cytochrome c in TBS (0.05 M Tris-HCl buffer, pH 7.6, containing 2% NaCl) was used as a blank. Samples were read at 550 nm and the results expressed as changes in OD per mg protein. Protein content was determined according to the Bradford method using bovine serum albumin (BSA) as a standard.

Serum lysozyme activity was evaluated as previously described (Balbi et al., 2014). To obtain hemolymph serum (*i.e.*, hemolymph free of cells), whole hemolymph was centrifuged at 200*g* for 10 min, and the supernatant was passed through a 0.22 µm filter. Lysozyme activity in aliquots of serum of hemocytes (control and exposed to $nCeO_2$) was determined spectrophotometrically at 450 nm utilizing *Micrococcus lysodeikticus*. Hen eggwhite (HEW) lysozyme was used as a concentration reference and lysozyme activity was expressed as HEW lysozyme equivalents (U/mL/mg protein). Protein content was determined according to the bicinchoninic acid (BCA) method using bovine serum albumin (BSA) as a standard. Data are expressed as U/mL/mg protein.

2.4. NO production in hemocytes and gills

Nitric oxide (NO) production by mussel hemocytes was evaluated as described previously (Balbi et al., 2014), by the Griess reaction, which quantifies the nitrite (NO_{2-}) content of supernatants. Aliquots of hemocyte suspensions (1.5 mL) were immediately frozen and stored at −80 °C until use. Before analysis, samples were thawed and centrifuged (12,000 *g* for 30 min at 4 °C), and the supernatants were analysed for NO_{2-} content. Aliquots (200 µL) in triplicate were incubated for 10 min in the dark with Griess reagent (1% Sulfanilamide, 0.1% N-(1- Naphthyl) ethylenediamine dihydrochloride, 5% H_3PO_4).

NO production in gills was evaluated using the same method as previously described (Della Torre et al., 2015). Gills were homogenized in 4 volumes of 0.05 M Tris buffer solution 2% NaCl, pH 7.6 and centrifuged at 1000 *g* for 15 min at 4 °C. The supernatants were then centrifuged at 16,900 *g* for 30 min and incubated for 2 h with the enzyme nitrate reductase in order to allow the reduction of nitrates to nitrites. After incubation, the following steps were the same as described above for hemocytes. Nitrite accumulation (nmol/mg prot/mL) was determined by a standard curve of known concentrations of sodium nitrite ($NaNO_2$).

2.5. Oxidative stress biomarkers in gills and digestive gland

Catalase (CAT) and Glutathione transferase (GST) were evaluated as previously described (Canesi et al., 2010; Barmo et al., 2013). Gills and digestive glands were homogenized respectively in 4 and 6 volumes of homogenization buffer (20 mM Tris buffer, 0.5 M sucrose, 0.15 M NaCl, pH 7.6) and centrifuged at 500 *g* for 15 min at 4 °C. The supernatants were then centrifuged at 14,000 *g* for 30 min. Both supernatant and pellet (containing mitochondria and peroxisomes) were utilized for the spectrophotometric evaluation of catalase activity following the decomposition of H_2O_2 at pH 7, 25 °C, at 240 nm (Viarengo et al., 1991). GSH transferase (GST) activity was evaluated on the supernatants with CDNB (1-chloro-2,4-dinitrobenzene) as a substrate. The formation of S-2,4-dinitro phenyl glutathione conjugate was evaluated by monitoring the increase in absorbance at 340 nm (Canesi and Viarengo, 1997). Enzyme activities were measured in triplicate readings for each sample. All data are reported as µmol/min/mg prot.

Lysosomal lipofuscin content in digestive gland tissue sections was determined as previously described (Canesi et al., 2010), using the Schmorl reaction on duplicate sections of 5 digestive glands (10 µm) using a Bright CM3050 cryostat, fixed in calcium–formaldehyde and rinsed with deionised water, followed by a 5 min incubation step with 1% Fe_2Cl_3, 1% potassium ferrocyanide in a 3:1 ratio (Moore, 1988). The sections were rinsed with 1% acetic acid and mounted in 20% (*v*/v) glycerol. Lipofuscin content were quantified by digital image analysis of stained sections and results are reported as % optical densities with respect to controls.

2.6. Gene expression

Total RNA was extracted from 6 pools of hemocytes and tissues obtained from each condition using TRIzol Reagent (Sigma, Milan, Italy) following the manufacturer's protocol. RNA concentration and quality were verified using the Qubit RNA assay (Thermo Fisher, Milan, Italy) and electrophoresis using a 1.5% agarose gel under denaturing conditions. First strand cDNA for each sample was synthesized from 1 µg total RNA (Balbi et al., 2014). Gene transcription was evaluated in 6 independent RNA samples. Primers pairs employed for qRT-PCR analysis were used as reported in previous studies (Table S2). qPCR reactions were performed in triplicate in a final volume of 15 µL containing 7.5 µL iTaq universal master mix with ROX (BioRad Laboratories, Milan, Italy), 5 µL diluted cDNA, and 0.3 mM specific primers (Table S2). A control lacking cDNA template (no-template) was included in the qPCR analysis to determine the specificity of target cDNA amplification. Amplifications were performed in a CFX96™ Real-Time PCR System (Biorad Italy, Segrate, Milan) using a standard “fast mode” thermal protocol. For each target mRNA, melting curves were utilized to verify the specificity of the amplified products and the absence of artefacts. Expression of 18 s was evaluated as reference gene, whose levels did not change in different experimental groups as previously described (Barmo et al., 2013). Expression of the genes of interest was then normalized using the expression levels of 18 s and the normalized expression was then reported as relative quantity of mRNA (relative expression) with respect to the control sample.

2.7. Determination of cerium content in exposure medium and tissues

Analytical determinations were performed by inductively coupled plasma mass spectrometry (ICP-MS) using a Perkin Elmer-Sciex ELAN DRC II (Concord, Ontario, Canada). The sample introduction system consisted of a PFA-ST (Elemental Scientific) joined with a low volume cyclonic spray chamber Cinnabar (Glass Expation). Determination of Ce was measured on the isotopes at *m/z* 140 and 142, which provided comparable results (within 2%). Each sample was analysed in triplicate, with a LOD = 2 µg/L. Total Cerium content (in µg/L) in exposure medium was evaluated at zero time and at different times post addition of $nCeO_2$ suspensions: after 2 and 12 h at day 1 (2 and 12 h), after 2 h and 12 h at day 4 (74 and 84 h). Samples were diluted 1:50 with 0.1% of 67% nitric acid (Ultrapur Normatom® from VWR). Three blanks were also prepared to check contamination. Total Cerium content (µg/g dw) in gills and digestive glands was evaluated on aliquots freeze-dried samples (100–250 mg) with a precision of ± 0.1 mg. Samples were digested with 1 mL of 65% nitric acid (Suprapur® from Merck), 3 mL of 30% hydrochloric acid (Suprapur® from Merck) and 1 mL of 30% hydrogen peroxide (Suprapur® from Merck), using the microwave digestion system MARS-5 (CEM, Matthews, NC, USA). Digestion was conducted for 50 min at 200 °C, with a high pressure containers Easy Prep Plus (1500 psi/300 °C, using 1600 W power). After cooling, samples were transferred into graduated flasks and diluted to 10 mL with Milli-Q water (Millipore, El Paso, TX, USA). Three blanks and CRMs (calcareous soil ERM - CC690 from the European Reference Materials) were also prepared to check contamination and analytical accuracy.

2.8. Embryotoxicity assay

Mussels sampled at the main spawning season (Feb-March 2017) were transferred to the laboratory and acclimatized in static tanks containing aerated artificial sea water (ASTM, 2004), pH 7.9–8.1,

36 ppt salinity (1 L/animal), at 16 ± 1 °C. Mussels were utilized within 2 days for gamete collection as previously described (Fabbri et al., 2014). When mussels beginning to spontaneously spawn were observed, each individual was immediately placed in a 250 mL beaker containing 200 mL of aerated ASW until complete gamete emission. After spawning, mussels were removed from beakers and sperms and eggs were sieved through 50 µm and 100 µm meshes, respectively, to remove impurities. Egg quality (shape, size) and sperm motility were checked using an inverted microscope. Eggs were fertilized with an egg:sperm ratio 1:10 in polystyrene 96-microwell plates (Costar, Corning Incorporate, NY, USA). After 30 min fertilization success (n. fertilized eggs/n. total eggs × 100) was verified by microscopical observation (> 85%).

The 48-h embryotoxicity assay (ASTM, 2004) was carried out in 96-microwell plates according to Fabbri et al. (2014). Aliquots of 20 µL of 10× suspensions of $nCeO_2$, suitably diluted in filter sterilized ASW, were added to fertilized eggs in each microwell to reach the nominal final concentrations (0–1000 µg/L for $nCeO_2$) in a 200 µL volume. Microplates were gently stirred for 1 min, and then incubated at 18 ± 1 °C for 48 h, with a 16 h:8 h light:dark photoperiod. At the end of the incubation time, samples were fixed with buffered formalin (4%). A larva was considered normal when the shell was D-shaped (straight hinge) and the mantle did not protrude out of the shell, and malformed if had not reached the stage typical for 48 h (trocophora or earlier stages) or when some developmental defects were observed (concave, malformed or damaged shell, protruding mantle). The recorded endpoint was the percentage of normal D-larvae in each well respect to the total, including malformed larvae and pre-D stages. The acceptability of test results was based on controls for a percentage of normal D-shell stage larvae > 75% (ASTM, 2004). Three experiments were made using 6 wells replicates per conditions. All larvae in each well were examined by optical microscopy using an inverted Olympus IX53 microscope (Olympus, Milano, Italy) at 400×, equipped with a CCD UC30 camera and a digital image acquisition software (cellSens Entry).

2.9. Statistics

Data, representing the mean ± SD of at least four samples in triplicate, were analysed by Mann-Whitney *U* test or by ANOVA followed by Tukey's *post hoc* test. For embryotoxicity test, data represent the mean ± SD of 3 independent experiments, carried out in 6 replicates in 96-microwell plates. All statistical analysis were performed using the PRISM 7 GraphPad software.

3. Results

3.1. Effects of $nCeO_2$ on immune and oxidative stress-related biomarkers in mussel hemolymph and tissues

The effects of $nCeO_2$ exposure on hemocytes and hemolymph functional parameters were first evaluated and the results are reported in Fig. 1. $nCeO_2$ did not affect LMS and phagocytic activity of mussel hemocytes (Fig. 1A and B); however, a significant increase in ROS production was observed (+25% with respect to controls, $P \leq 0.05$) (Fig. 1C). Moreover, $nCeO_2$ induced a large increase in serum lysozyme activity (about +50% with respect to controls, $P \leq 0.05$) (Fig. 1D). $nCeO_2$ did not increase NO production in either circulating hemocytes and gills, evaluated as a possible marker of inflammation at the cellular and tissue level (Fig. S1).

In contrast, significant effects of $nCeO_2$ exposure were observed on the activities of Catalase and GST in both gills and digestive gland (Fig. 2). Catalase activity was increased (about +45% in gills and +19% in digestive gland with respect to controls, $P \leq 0.05$) (Fig. 2A and B). In the digestive gland, but not in gills, stimulation of GST activity was also observed (about +28%, $P \leq 0.05$) (Fig. 2C and D). Moreover, when lysosomal lipofuscin accumulation was evaluated in this tissue as a biomarker of lipid peroxidation, a drastic decrease was observed in $nCeO_2$-exposed samples (−63% with respect to controls; $P \leq 0.05$) (Fig. 3).

3.2. Effects on gene expression in hemocytes and digestive gland

Transcription of selected genes related to different biological functions, antioxidant defense and detoxification response (superoxide dismutase-SOD, catalase-CAT, glutathione-s-transferase-GST, metallothionein isoforms 10 and 20 - MT10 and MT20), neuroendocrine signaling (serotonin receptor, 5- HTR), immune response (lysozyme, Mytilin B, MytB, Myticin B, MytC, C1q-domain-containing protein-MgC1q, Toll-like receptor-TLR-i), was evaluated by RT-q-PCR in both hemocytes and digestive gland of control and $nCeO_2$-exposed mussels. Data on relative expression of each transcript (fold changes with respect to control) are reported in Fig. 3A. To help comparing overall transcript levels among datasets, fold change variations of target transcripts are also reported into a graphical representation using a heatmap (Fig. 4B).

The results obtained in hemocytes indicate that expression of 4 out of 11 gene transcripts was significantly modulated by exposure to $nCeO_2$, all of which were significantly up-regulated (Fig. 4A). Expression of 5-HTR and Lysozyme showed a three-and four-fold increase with respect to controls, respectively ($P \leq 0.05$). A large increase in mRNA levels for MT20 and, to a lesser extent, for MT10, was also recorded (four-fold and + 57%; $P \leq 0.05$). A distinct effect was observed in the digestive gland, with downregulation of 2 genes; the antimicrobial peptide MytB and the MT20 isoform (−57 and −48% with respect to controls; $P \leq 0.05$). In contrast, transcription of MT10 was significantly increased (+40%; $P \leq 0.05$).

3.3. Cerium concentration in exposure medium and in mussel tissues

Cerium (Ce) concentrations in exposure medium were evaluated by ICP-MS in whole ASW samples collected at different times pre- and

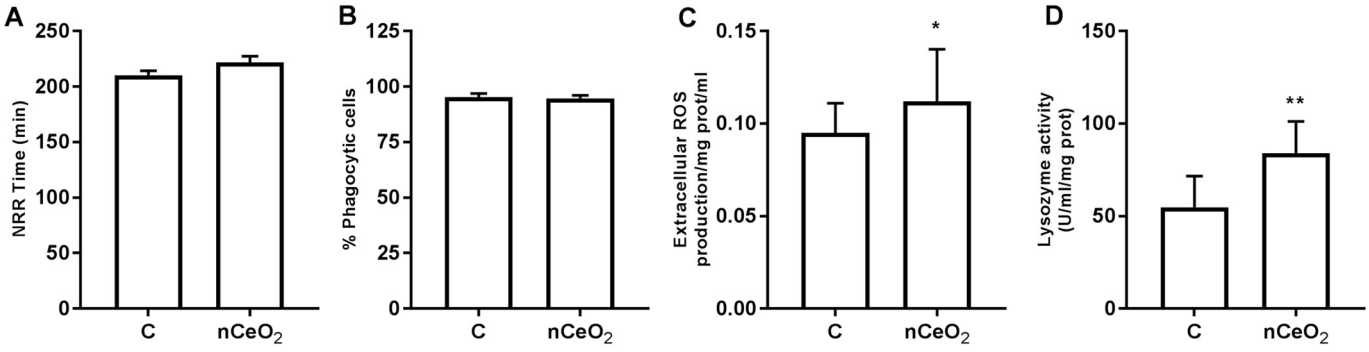

Fig. 1. Effects of $nCeO_2$ exposure (100 µg/L, 96 h) on *Mytilus galloprovincialis* hemocytes. A) Lysosomal membrane stability-LMS; B) phagocytic activity; C) extracellular ROS production; D) extracellular lysozyme release. Data are reported as mean (N = 4) ± SD. *P < 0.05, **P < 0.01 (Mann-Whitney *U* test).

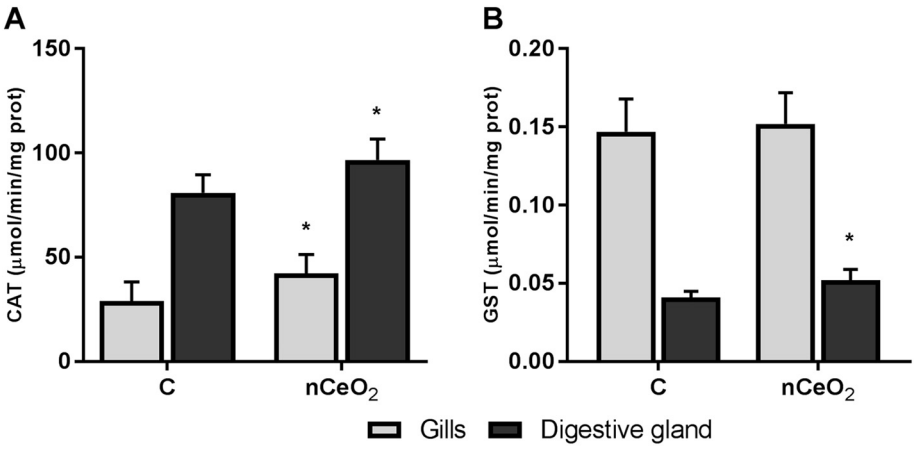

Fig. 2. Effect of $nCeO_2$ exposure (100 µg/L, 96 h) on *Mytilus galloprovincialis* antioxidant enzyme activities in gills (grey) and digestive gland (black). A) Catalase (CAT); B) Glutathione-S-transferase (GST). Data, representing the mean ± SD (N = 4), are expressed as µmol/min/mg prot. For each tissue, significant differences observed with respect to control are indicated * P < 0.05 (Mann-Whitney U test).

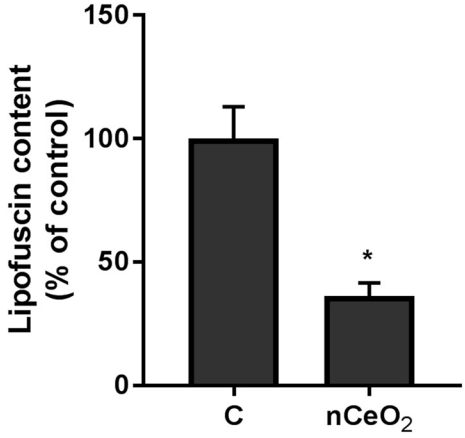

Fig. 3. Effect of $nCeO_2$ exposure (100 µg/L, 96 h) on *Mytilus galloprovincialis* lysosomal lipofuscin content in digestive gland. Data are reported as mean ± SD (N = 4). *P < 0.05 (Mann-Whitney U test).

post-addition of $nCeO_2$ at day 1 and day 4 of exposure as previously described in experiments with $nTiO_2$ (Balbi et al., 2014). As shown in Fig. S2, Ce concentrations detected 2 h after addition of $nCeO_2$ both at day 1 and day 4 were 24.5 ± 2.8 µg/L and 34.8 ± 3.5 µg/L, representing 26 and 42%, respectively, of the nominally added Ce (about 80 µg/L Ce in 100 µg/L $nCeO_2$ on a mass basis). This indicates that, although some $nCeO_2$ may be rapidly taken up by the mussels, a significant and fairly constant fraction was available in suspension in exposure medium throughout the experiment. However, when at the end of exposure (96 h) tissue Ce concentrations were evaluated, no differences were observed in gills and digestive glands of control and exposed mussels (about 0.5 ± 0.03 and 1 ± 0.08 µg/g dw respectively), indicating no tissue accumulation.

3.4. Effects on embryo development

Fertilized eggs were exposed to different concentrations (from 0.01 to 1000 µg/L) of $nCeO_2$ in 96-microwell plates, and the percentage of normal D-larvae was evaluated after 48 hpf as previously described (Fabbri et al., 2014; Balbi et al., 2017). The results, reported in Fig. 5, show that $nCeO_2$ induced a slight decrease in normal larval development. No concentration dependent effects were observed in the range of 1–1000 µg/L, with small decreases in percentage of normal D-larvae that were maximal at the highest concentration tested (−17%; $P \leq 0.05$). Exposure to $nCeO_2$ resulted in malformations of D-veligers, generally represented by deformations of the shell hinge line (inset).

4. Discussion

The results indicate that *in vivo* exposure of *M. galloprovincialis* to $nCeO_2$ elicited significant changes in physiological parameters related to the immune function and antioxidant defense, from molecular to cell/tissue level.

In this work, for *in vivo* experiments, we utilized a type of $nCeO_2$ that was previously shown to exert distinct immune and redox properties on mussel hemocytes *in vitro*, in the presence of hemolymph serum in comparison with ASW as exposure medium (Canesi et al.,

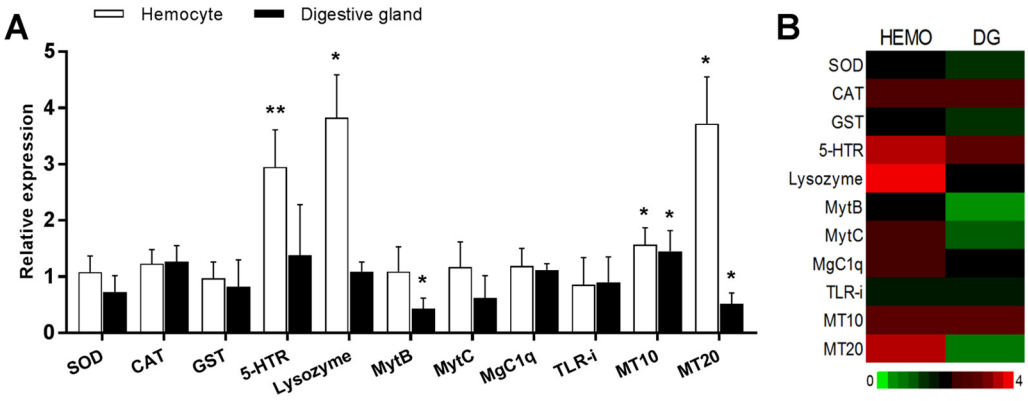

Fig. 4. Effect of $nCeO_2$ exposure (100 µg/L, 96 h) on gene transcription in *Mytilus galloprovincialis* hemocytes (white) and digestive gland (black). A) Relative expression of SOD (superoxide dismutase), CAT (catalase), GST (glutathione transferase), 5-HTR (5-hydroxyl triptamine receptor), lysozyme, MytB (Mytilin B), MytC (Myticin B), MgC1q (C1q-domain-containing protein), TLR-i (Toll-like receptor i isoform), MT10 (metallothionein isoform 10), MT20 (metallothionein isoform 20). B) Heatmap of 11 differentially expressed genes was generated in each sample. Data are reported as mean ± SD of the relative expression with respect to untreated samples within each tissue (N = 6). *P < 0.05, (Mann-Whitney U test).

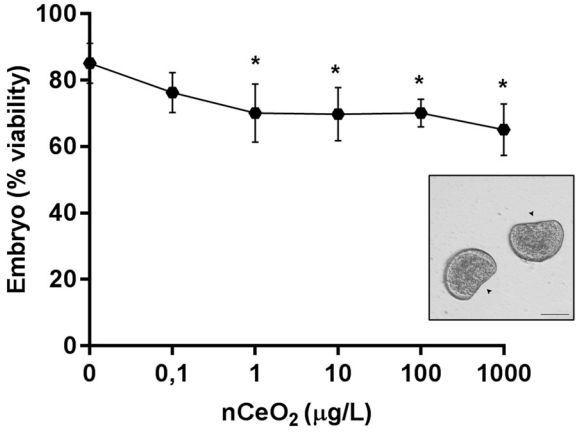

Fig. 5. Effects of $nCeO_2$ on *M. galloprovincialis* larval development evaluated in the 48 h embryotoxicity assay. Fertilized eggs were exposed to different concentrations of $nCeO_2$ in ASW (0.01–1000 µg/L). Data, expressed as percentage of normal D-shaped larvae with respect to controls the mean ± SD of 3 experiments carried out in 96-multiwell plates (6 replicate wells for each sample). Inset: Representative light microscopy images of $nCeO_2$-exposed embryos (1000 µg/L). Scale bar: 20 µm.

2017; Sendra et al., 2018). *In vivo* exposure conditions were chosen according to previous studies on $nCeO_2$ in bivalves (Montes et al., 2012; Conway et al., 2014; Garaud et al., 2015), and also in comparison to extensive *in vivo* data obtained in mussels with another nano-oxide, $nTiO_2$ (Barmo et al., 2013; Balbi et al., 2014; Della Torre et al., 2015; Banni et al., 2016).

The results here obtained show that several biomarkers at molecular, cellular and tissue level were affected by *in vivo* exposure to $nCeO_2$. In particular, specific immune and antioxidant responses were observed. In hemocytes, $nCeO_2$ did not affect LMS or phagocytic activity, whereas the most striking response was the increase in hemolymph lysozyme activity. Extracellular ROS production was increased in hemocytes, but no effects were observed on NO production in either hemocytes or gills, suggesting the absence of inflammatory processes. The immunomodulatory effects on hemocytes were distinct from those previously observed *in vitro*. This discrepancy could be partly due to the obvious differences in exposure conditions *in vitro* and *in vivo* (concentrations and times of exposure). However, the overall impact observed *in vivo* would result from particle behavior in both external and internal media, thus better reflecting the potential environmental exposure conditions (Canesi and Corsi, 2016; Canesi et al., 2017).

At the tissue level, increased antioxidant enzyme activities were recorded, in particular in the digestive gland. Moreover, in this tissue, exposure to $nCeO_2$ induced a large decrease in lysosomal accumulation of lipofuscin. Lipofuscin accumulation, which represents the final product of lipid peroxidation processes, is generally increased in mussels by exposure to pollutants, including NPs (Canesi et al., 2010); to our knowledge, this is the first report of a net reduction of this biomarker of oxidative stress in response to contaminant exposure. Taken together, the results demonstrate that in *Mytilus* $nCeO_2$ exerts antioxidant effects at the tissue level. The results reinforce and extend previous observations with other types of to $nCeO_2$ in the freshwater bivalve *D. polymorpha* (Garaud et al., 2015).

In order to identify the molecular mechanisms possibly underlying the functional responses induced by $nCeO_2$ in mussel hemocytes and digestive gland, that apparently represented the main targets for $nCeO_2$, transcription profiles of 11 genes involved in different biological processes were evaluated. The results indicate a cell/tissue distinct pattern of gene transcription. In hemocytes, upregulation of immune and antioxidant-related genes was observed. In particular, the level of mRNA for lysozyme was largely increased, in line with the increased activity observed in the hemolymph. Lysozyme represents a key element in both humoral and cellular immune response of mussels (Canesi et al., 2002). Interestingly, $nCeO_2$ has been recently shown to interact with the molecular structure of hen egg-white lysozyme *in vitro*, possibly affecting its activity (Cheng et al., 2017). In this light, the observed increases in lysozyme activity and expression may be partly interpreted as a compensatory response to $nCeO_2$ exposure.

Moreover, $nCeO_2$ induced upregulation of both MT isoforms MT20 and MT10. MTs are sulfhydryl rich protein involved in heavy metal homeostasis and antioxidant defense; in *Mytilus*, MT20 is preferentially induced in presence of toxic metals and oxidative stress conditions, while MT10 represents the constitutive form engaged in cellular homeostasis of essential metals (Dondero et al., 2006; Vergani et al., 2007). The results underline how $nCeO_2$ can upregulate non enzymatic antioxidant defenses in mussel hemocytes. These are the first data on the effects of $nCeO_2$ on MT transcription not only in marine invertebrates, but also in higher organisms. In mice, administration of Ce (III) induced hepatic MTs; the effect was apparently mediated by indirect mechanism where interleukin 6 played a key role; moreover, the metal bound to MTs was not Cerium but Zinc (Kobayashi et al., 2006). Unfortunately, from our first data, to draw any mechanistic relationship between $nCeO_2$ exposure and MT induction is purely speculative.

In the digestive gland, minor changes in gene transcription were observed, with a general decreasing pattern in response to $nCeO_2$ exposure, except for a small but significant upregulation of MT10.

Finally, a large increase in transcription of the serotonin receptor 5-HTR was observed in the hemocytes, as well a slight increase, although not significant, in the digestive gland. Previous work on zebrafish embryos showed a negative interaction of nanoceria with neuroendocrine signaling related to serotonin, suggesting that $nCeO_2$ may thus decrease the amount of 5-HT available for normal cell functioning (Özel et al., 2013). In mussel hemocytes, increased transcription of 5-HTR might compensate for a lower ligand availability in the surrounding media. In bivalves, serotonin modulates various biological processes such as feeding, immunity, and response to a variety of stressors, including contaminant exposure (Ciacci et al., 2011; Dong et al., 2017). However, the effects and mechanisms of action of NPs on neuroendocrine signaling are scarce in aquatic organisms and almost absent in bivalves. The sole increase in mRNA levels for 5-HTR induced by $nCeO_2$ is only indicative of possible alterations in physiological serotonin signaling. The possible impact of $nCeO_2$ on neuroendocrine physiology of mussels requires further investigation.

Data on physiological responses to nanoceria are available in freshwater bivalves in experimental conditions similar to those of the present study. In the digestive gland of *D. polymorpha*, exposure to $nCeO_2$ led to decreases in the size of the lysosomal system, catalase activity and lipoperoxidation in the digestive gland, but also negatively impacted hemolymph ion concentrations (Garaud et al., 2015). In the same tissue of the clam *Corbicula fluminea*, significant induction of caspase pathway and DNA damage were observed (Koehlé-Divo et al., 2018). The results may be due to species-specific responses, as well as to the type of nanoceria.

Overall, the results indicate that $nCeO_2$ induces immune and antioxidant responses in the marine mussel *Mytilus*. To best of our knowledge, this is the first study on the physiological responses of marine bivalves to nanoceria. Moreover, the results on gene transcription represent the first data on the possible molecular targets for $nCeO_2$ in marine invertebrate cells and tissues.

The immunomodulatory and antioxidant effects of NPs, and in particular of nanoceria, have been recently discussed (Casals et al., 2017) in relation to the modifications occurring in exposure media in which the NPs are dispersed. These include agglomeration and aggregation, formation of the NP protein corona, and NP corrosion and/or dissolution into ionic species, which is low for $nCeO_2$ (Singh et al., 2014). In the present work, both particle behavior in ASW and in mussel biological fluid (hemolymph serum), as well as formation of a SOD protein corona (Canesi et al., 2017) were taken into account in

order to understand the biological effects observed.

However, the correlation between the impact of nanoceria and its behavior in exposure media, uptake and bioaccumulation, are still far to be understood in bivalves. As suspension feeders, capture and ingestion of NPs is enhanced by aggregation/agglomeration (Ward and Kach, 2009; Canesi et al., 2012). Different types of $nCeO_2$ have been shown to form agglomerates of different sizes in freshwater and marine exposure media (this work, Conway et al., 2014; Garaud et al., 2015; Koehlé-Divo et al., 2018). However, Montes et al. (2012) showed that in *M. galloprovincialis* exposed to $nCeO_2$, almost all of the Ce mass was removed from the water column after 24 h of exposure and it was mainly transferred in pseudo-feces, with a low Ce accumulation in the whole organism (1–3%). In the same species, approximately 99% of CeO_2 was captured and excreted in pseudo-feces, and average pseudo-feces mass doubled in response to CeO_2 exposure (Conway et al., 2014). In *D. polymorpha*, estimated accumulation of the total introduced Ce was 2.4% (Garaud et al., 2015). Our data indicate that the Ce concentration in the water column was relatively constant throughout the experiment, representing about 30% of the nominal added concentration. Although whether the remaining fraction was taken up by the mussels or sedimented as aggregates of $nCeO_2$ was not determined in the present study, no significant accumulation of Ce could be detected in either gills and digestive gland, as previously shown in the digestive gland of *C. fluminea* (Koehlé-Divo et al., 2018). A possible explanation is that the mussels may perceive $nCeO_2$ as being inedible, and increase pseudo-feces production to capture and reject most of the NPs. However, a transient entrance of $nCeO_2$ in tissues occurred within the time of exposure (Koehlé-Divo et al., 2018). Distribution, transport and relocating of $nCeO_2$ in organisms seem to be run by temporal factors. Conway et al. (2014) noticed that $nCeO_2$ seems to be temporarily stored in the digestive system or elsewhere in the organism, as it was not immediately captured in pseudo-feces.

Overall, despite the little potential for $nCeO_2$ bioaccumulation in bivalve tissues, the results here obtained demonstrate that this type of NPs are able to elicit significant biological effects at molecular, cellular and tissue level. On the basis of these results, a tentative scheme of $nCeO_2$ interaction in mussels can be drawn. The stronger effects of $nCeO_2$ on gene expression observed in hemocytes suggest that some particles (or their agglomerates) may directly enter the open circulatory system of the mussel through the gills or extrapallial fluid and activate circulating hemocytes. These cells, that represent the first line of defense against foreign particles, would respond with multiple defense mechanisms, including lysozyme release, extracellular ROS production, and upregulation of immune and antioxidant genes. However, this would not result in oxidative stress or inflammatory processes, since $nCeO_2$ interactions with soluble SOD in the hemolymph and formation of a $nCeO_2$-protein corona may increase SOD activity (Canesi et al., 2017), as in mammalian systems (Korsvik et al., 2007). Production of H_2O_2 by extracellular SOD in circulating fluid would in turn stimulate antioxidant enzyme activities in the tissues, this leading to decreased oxidative stress conditions, as indicated by the drop in lysosomal lipofuscin content in the digestive gland. Transient interactions of $nCeO_2$ through the digestive system could also contribute to the antioxidant effect observed in the digestive gland.

A distinct scenario has been hypothesized with another type of nano-oxide, $nTiO_2$ in the same experimental conditions (Canesi et al., 2010, 2014; Barmo et al., 2013; Balbi et al., 2014; Della Torre et al., 2015; Banni et al., 2016). Although $nTiO_2$ in ASW formed agglomerates of comparable size with those of $nCeO_2$, no protein corona was formed in the hemolymph (Canesi et al., 2017). Moreover, significant accumulation of Ti was observed in mussel tissues (Balbi et al., 2014; Della Torre et al., 2015). Accordingly, $nTiO_2$ exerted several effects in gills and digestive gland, including inflammation and changes in lysosomal and oxidative stress biomarkers. In the hemocytes, $nTiO_2$ induced lysosomal damage and pre-apoptotic processes, together with inhibition of phagocytosis and increased ROS and NO production. The immunomodulatory effects observed in hemocytes were ascribed, as indicated for other NPs (Browne et al., 2008) to transfer from digestive cells to hemolymph (Barmo et al., 2013; Balbi et al., 2014; Canesi et al., 2010). Finally, transcriptional changes induced by $nTiO_2$ in both digestive gland and hemocytes were distinct from those observed in the present work with $nCeO_2$. Overall, the results further underline the specificity of mussel response to *in vivo* exposure to nano-oxides.

Finally, the possible impact of $nCeO_2$ was also investigated at the organism level, on early life stages of *M. galloprovincialis*, that have been shown to represent a sensitive target for certain types of NPs (Balbi et al., 2017; Auguste et al., 2018). $nCeO_2$ showed limited effects on embryo development, probably due to increasing agglomeration at increasing concentrations. However, maximal agglomeration in ASW was observed at 48 h at 1 mg/L $nCeO_2$ (Table S1), corresponding to the maximal concentration utilized in the embryotoxiciy assay. At the lower concentrations tested in most experiments (from 0.1 to 100 µg/L), the size of agglomerates is expected to be much lower, since agglomeration also depend on particle concentration. Moreover, although the obtained data indicate a small impact of $nCeO_2$ on embryo development, the results obtained in this work can contribute to the evaluation of the potential embryotoxicity of different types of NPs when compared with previous data obtained in the same experimental conditions with other NP types with different core composition, physico chemical characteristics and behavior in ASW. According to these data, $nTiO_2$ was ineffective (Balbi et al., 2014), AgNPs moderately embryotoxic (Auguste et al., 2018), polystyrene amino modified NPs-$PSNH_2$ strongly embryotoxic (Balbi et al., 2017). In this light, the embryotoxicity of different types of NPs in mussels are $nTiO_2 < nCeO_2 < AgNPs < PSNH_2$. With regards to the effects of $nCeO_2$, essentially consisting in shell hinge malformations, these may be ascribed to interference of $nCeO_2$ with the mechanisms involved in bivalve shell formation. Among these, tyrosinase, an enzyme that participates in secretion of the shell organic matrix (Huan et al., 2013) and shows phenol oxidase mimicking activities (Hayat et al., 2015), may be affected by exposure to nanoceria. These data would further support the redox mechanisms at the basis of the physiological effects of $nCeO_2$ in aquatic invertebrates. Overall, the results demonstrate that in mussels $nCeO_2$ can selectively modulate different physiological processes at the cellular, tissue and organism level, confirming the antioxidant and immunomodulatory properties of this type of NPs.

Funding

This project has received funding from the European Union's Horizon 2020 research and innovation programme under the Marie Skłodowska-Curie grant agreement PANDORA N° 671881.

Conflict of interest

The authors report no conflicts of interest in this work.

Appendix A. Supplementary data

Supplementary data to this article can be found online at https://doi.org/10.1016/j.cbpc.2019.02.006.

References

ASTM, 2004. Standard Guide for Conducting Static Acute Toxicity Tests Starting with Embryos of Four Species of Saltwater Bivalve Molluscs.

Auguste, M., Ciacci, C., Balbi, T., Brunelli, A., Caratto, V., Marcomini, A., Cuppini, R., Canesi, L., 2018. Effects of nanosilver on *Mytilus galloprovincialis* hemocytes and early embryo development. Aquat. Toxicol. 203, 107–116.

Balbi, T., Smerilli, A., Fabbri, R., Ciacci, C., Montagna, M., Grasselli, E., Brunelli, A., Pojana, G., Marcomini, A., Gallo, G., Canesi, L., 2014. Co-exposure to n-TiO_2 and Cd^{2+} results in interactive effects on biomarker responses but not in increased toxicity in the marine bivalve *M. galloprovincialis*. Sci. Total Environ. 493, 355–364.

Balbi, T., Camisassi, G., Montagna, M., Fabbri, R., Franzellitti, S., Carbone, C., Dawson,

K., Canesi, L., 2017. Impact of cationic polystyrene nanoparticles (PS-NH_2) on early embryo development of *Mytilus galloprovincialis*: effects on shell formation. Chemosphere 186, 1–9.
Banni, M., Sforzini, S., Balbi, T., Corsi, I., Viarengo, A., Canesi, L., 2016. Combined effects of n-TiO_2 and 2,3,7,8-TCDD in *Mytilus galloprovincialis* digestive gland: a transcriptomic and immunohistochemical study. Environ. Res. 145, 135–144.
Barmo, C., Ciacci, C., Canonico, B., Fabbri, R., Cortese, K., Balbi, T., Marcomini, A., Pojana, G., Gallo, G., Canesi, L., 2013. In vivo effects of n-TiO_2 on digestive gland and immune function of the marine bivalve *Mytilus galloprovincialis*. Aquat. Toxicol. 132–133, 9–18.
Browne, M.A., Dissanayake, A., Galloway, T.S., Lowe, D.M., Thompson, R.C., 2008. Ingested microscopic plastic translocates to the circulatory system of the mussel, *Mytilus edulis* (L.). Environ. Sci. Technol. 42, 5026–5031.
Canesi, L., Corsi, I., 2016. Effects of nanomaterials on marine invertebrates. Sci. Total Environ. 565, 933–940.
Canesi, L., Viarengo, A., 1997. Age-related differences in glutathione metabolism in mussel tissues (*Mytilus edulis* L). Comp. Biochem. Physiol. B 116, 217–221.
Canesi, L., Gallo, G., Gavioli, M., Pruzzo, C., 2002. Bacteria-hemocyte interactions and phagocytosis in marine bivalves. Microsc. Res. Tech. 57, 469–476.
Canesi, L., Fabbri, R., Gallo, G., Vallotto, D., Marcomini, A., Pojana, G., 2010. Biomarkers in *Mytilus galloprovincialis* exposed to suspensions of selected nanoparticles (Nano carbon black, C60 fullerene, Nano-TiO_2, Nano-SiO_2). Aquat. Toxicol. 100, 168–177.
Canesi, L., Ciacci, C., Fabbri, R., Marcomini, A., Pojana, G., Gallo, G., 2012. Bivalve molluscs as a unique target group for nanoparticle toxicity. Mar. Environ. Res. 76, 16–21.
Canesi, L., Frenzilli, G., Balbi, T., Bernardeschi, M., Ciacci, C., Corsolini, S., Della Torre, C., Fabbri, R., Faleri, C., Focardi, S., Guidi, P., Kočan, A., Marcomini, A., Mariottini, M., Nigro, M., Pozo-Gallardo, K., Rocco, L., Scarcelli, V., Smerilli, A., Corsi, I., 2014. Interactive effects of n-TiO_2 and 2,3,7,8-TCDD on the marine bivalve *Mytilus galloprovincialis*. Aquat. Toxicol. 153, 53–65.
Canesi, L., Balbi, T., Fabbri, R., Salis, A., Damonte, G., Volland, M., Blasco, J., 2017. Biomolecular coronas in invertebrate species: implications in the environmental impact of nanoparticles. NanoImpact 8, 89–98.
Casals, E., Gusta, M.F., Piella, J., Casals, G., Jiménez, W., Puntes, V., 2017. Intrinsic and extrinsic properties affecting innate immune responses to nanoparticles: the case of cerium oxide. Front. Immunol. 8, 970.
Celardo, I., Pedersen, J.Z., Traversa, E., Ghibelli, L., 2011. Pharmacological potential of cerium oxide nanoparticles. Nanoscale 3, 1411.
Cheng, Y.-H., Lai, C.-M., Lin, K.-S., Wang, S.S.-S., 2017. Effects of metal oxide nanoparticles on the structure and activity of lysozyme. Colloid. Surf. B 151, 344–353.
Ciacci, C., Barmo, C., Fabbri, R., Canonico, B., Gallo, G., Canesi, L., 2011. Immunomodulation in *Mytilus galloprovincialis* by non-toxic doses of hexavalent Chromium. Fish Shellfish Immunol. 31, 1026–1033.
Ciacci, C., Canonico, B., Bilaničová, D., Fabbri, R., Cortese, K., Gallo, G., Marcomini, A., Pojana, G., Canesi, L., 2012. Immunomodulation by different types of N-oxides in the hemocytes of the marine bivalve *Mytilus galloprovincialis*. PLoS One 7, e36937.
Collin, B., Oostveen, E., Tsyusko, O.V., Unrine, J.M., 2014. Influence of natural organic matter and surface charge on the toxicity and bioaccumulation of functionalized ceria nanoparticles in *Caenorhabditis elegans*. Environ. Sci. Technol. 48, 1280–1289.
Conway, J.R., Hanna, S.K., Lenihan, H.S., Keller, A.A., 2014. Effects and implications of trophic transfer and accumulation of CeO_2 nanoparticles in a marine mussel. Environ. Sci. Technol. 48, 1517–1524.
Della Torre, C., Balbi, T., Grassi, G., Frenzilli, G., Bernardeschi, M., Smerilli, A., Guidi, P., Canesi, L., Nigro, M., Monaci, F., Scarcelli, V., Rocco, L., Focardi, S., Monopoli, M., Corsi, I., 2015. Titanium dioxide nanoparticles modulate the toxicological response to cadmium in the gills of *Mytilus galloprovincialis*. J. Hazard. Mater. 297, 92–100.
Dondero, F., Placentini, L., Banni, M., Rebelo, M., Burlando, B., Viarengo, A., 2006. Quantitative PCR analysis of two molluscan metallothionein genes unveils differential expression and regulation. Gene 345, 259–270.
Dong, W., Liu, Z., Qiu, L., Wang, W., Song, X., Wang, X., Li, Y., Xin, L., Wang, L., Song, L., 2017. The modulation role of serotonin in Pacific oyster *Crassostrea gigas* in response to air exposure. Fish Shellfish Immunol. 62, 341–348.
Fabbri, R., Montagna, M., Balbi, T., Raffo, E., Palumbo, F., Canesi, L., 2014. Adaptation of the bivalve embryotoxicity assay for the high throughput screening of emerging contaminants in *Mytilus galloprovincialis*. Mar. Environ. Res. 99, 1–8.
Garaud, M., Trapp, J., Devin, S., Cossu-Leguille, C., Pain-Devin, S., Felten, V., Giamberini, L., 2015. Multibiomarker assessment of cerium dioxide nanoparticle ($nCeO_2$) sublethal effects on two freshwater invertebrates, *Dreissena polymorpha* and *Gammarus roeseli*. Aquat. Toxicol. 158, 63–74.
Gottschalk, F., Lassen, C., Kjoelholt, J., Christensen, F., Nowack, B., 2015. Modeling flows and concentrations of nine engineered nanomaterials in the Danish environment. Int. J. Environ. Res. Public Health 12, 5581–5602.
Hayat, A., Cunningham, J., Bulbul, G., Andreescu, S., 2015. Evaluation of the oxidase like activity of nanoceria and its application in colorimetric assays. Anal. Chim. Acta 885, 140–147.
Huan, P., Liu, G., Wang, H., Liu, B., 2013. Identification of a tyrosinase gene potentially involved in early larval shell biogenesis of the Pacific oyster *Crassostrea gigas*. Dev. Genes Evol. 223, 389–394.
Kobayashi, K., Kuroda, J., Shibata, N., Hasegawa, T., Seko, Y., Satoh, M., Tohyama, C., Takano, H., Imura, N., Sakabe, K., Fujishiro, H., Himeno, S., 2006. Induction of metallothionein by manganese is completely dependent on Interleukin-6 production. J. Pharmacol. Exp. Ther. 320, 721–727.
Koehlé-Divo, V., Cossu-Leguille, C., Pain-Devin, S., Simonin, C., Bertrand, C., Sohm, B., Mouneyrac, C., Devin, S., Giambérini, L., 2018. Genotoxicity and physiological effects of CeO_2 NPs on a freshwater bivalve (*Corbicula fluminea*). Aquat. Toxicol. 198, 141–148.
Korsvik, C., Patil, S., Seal, S., Self, W.T., 2007. Superoxide dismutase mimetic properties exhibited by vacancy engineered ceria nanoparticles. Chem. Commun. 1056.
Li, C., Shi, X., Shen, Q., Guo, C., Hou, Z., Zhang, J., 2018. Hot topics and challenges of regenerative nanoceria in application of antioxidant therapy. J. Nanomater. 2018, 1–12.
Montes, M.O., Hanna, S.K., Lenihan, H.S., Keller, A.A., 2012. Uptake, accumulation, and biotransformation of metal oxide nanoparticles by a marine suspension-feeder. J. Hazard. Mater. 225–226, 139–145.
Moore, M., 1988. Cytochemical responses of the lysosomal system and NADPH-ferrihemoprotein reductase in molluscan digestive cells to environmental and experimental exposure to xenobiotics. Mar. Ecol. Prog. Ser. 46, 81–89.
MRR 2017, Market Research Report, Grand View Research, Cerium Oxide Nanoparticles Market Size, Industry Report, 2018–2025, https://www.grandviewresearch.com/industry-analysis/cerium-oxide-nanoparticles-market, (last access 09/11/2018).
Nelson, B., Johnson, M., Walker, M., Riley, K., Sims, C., 2016. Antioxidant cerium oxide nanoparticles in biology and medicine. Antioxidants 5, 15.
O'Brien, N., Cummins, E., 2010. Ranking initial environmental and human health risk resulting from environmentally relevant nanomaterials. J. Environ. Sci. Health A 45 (8), 992–1007.
Özel, R.E., Hayat, A., Wallace, K.N., Andreescu, S., 2013. Effect of cerium oxide nanoparticles on intestinal serotonin in zebrafish. RSC Adv. 3, 15298.
Rajeshkumar, S., Naik, P., 2018. Synthesis and biomedical applications of cerium oxide nanoparticles – a review. Biotechnol. Rep. 17, 1–5.
Reed, K., Cormack, A., Kulkarni, A., Mayton, M., Sayle, D., Klaessig, F., Stadler, B., 2014. Exploring the properties and applications of nanoceria: is there still plenty of room at the bottom? Environ. Sci. Nano 1, 390–405.
Sendra, M., Yeste, P.M., Moreno-Garrido, I., Gatica, J.M., Blasco, J., 2017. CeO_2 NPs, toxic or protective to phytoplankton? Charge of nanoparticles and cell wall as factors which cause changes in cell complexity. Sci. Total Environ. 590–591, 304–315.
Sendra, M., Volland, M., Balbi, T., Fabbri, R., Yeste, M.P., Gatica, J.M., Canesi, L., Blasco, J., 2018. Cytotoxicity of CeO_2 nanoparticles using in vitro assay with *Mytilus galloprovincialis* hemocytes: relevance of zeta potential, shape and biocorona formation. Aquat. Toxicol. 200, 13–20.
Singh, C., Gibson, N., Levin, M., Friedrichs, S., Ceccone, G., Goenaga Infante, H., Rasmussen, K., Alstrup Jensen, K., Carlander, D., 2014. Institute for Health Consumer Protection. In: Cerium Dioxide NM-211, NM- 212, NM-213, Characterisation and Test Item Preparation JRC Repository: NM-series of Representative Manufactured Nanomaterials. Publications Office of the European Union, Luxembourg. https://doi.org/10.2788/80203.
Taylor, N.S., Merrifield, R., Williams, T.D., Chipman, J.K., Lead, J.R., Viant, M.R., 2015. Molecular toxicity of cerium oxide nanoparticles to the freshwater alga *Chlamydomonas reinhardtii* is associated with supra-environmental exposure concentrations. Nanotoxicology 1–10.
Vergani, L., Grattarola, M., Grasselli, E., Dondero, F., Viarengo, A., 2007. Molecular characterization and function analysis of MT-10 and MT-20 metallothionein isoforms from *Mytilus galloprovincialis*. Arch. Biochem. Biophys. 465, 247–253.
Viarengo, A., Canesi, L., Pertica, M., Livingstone, D.R., 1991. Seasonal variation of antioxidant defence systems and lipid peroxidation in the digestive gland of mussels. Comp. Biochem. Physiol. C 187–190.
Ward, J.E., Kach, D.J., 2009. Marine aggregates facilitate ingestion of nanoparticles by suspension feeding bivalves. Mar. Environ. Res. 68, 137–142.
Xia, T., Kovochich, M., Liong, M., Mädler, L., Gilbert, B., Shi, H., Yeh, J.I., Zink, J.I., Nel, A.E., 2008. Comparison of the mechanism of toxicity of zinc oxide and cerium oxide nanoparticles based on dissolution and oxidative stress properties. ACS Nano 2, 2121–2134.
Yokel, R.A., Hussain, S., Garantziotis, S., Demokritou, P., Castranova, V., Cassee, F.R., 2014. The yin: an adverse health perspective of nanoceria: uptake, distribution, accumulation, and mechanisms of its toxicity. Environ. Sci. Nano 1, 406–428.